Microfluid Nanofluid (2009) 7:383–392
DOI 10.1007/s10404-008-0390-5

RESEARCH PAPER

Electrophoresis of a finite rod along the axis of a long cylindrical microchannel filled with Carreau fluids

Li-Hsien Yeh · Jyh-Ping Hsu

Received: 23 September 2008 / Accepted: 4 December 2008 / Published online: 8 January 2009

Abstract The boundary effect on the electrophoretic behavior of a particle in a non-Newtonian fluid is studied by considering the electrophoresis of a finite rod along the axis of a cylindrical microchannel filled with shear-thinning Carreau fluids, which include both Newtonian and power-law fluids as special cases. Under the conditions of low surface potential and weak applied electric field, the influences of the radius of the microchannel, the aspect ratio of the rod, the thickness of double layer, and the nature of the Carreau fluid on the mobility of the rod are investigated. We show that due to the shear-thinning effect, the mobility of the rod in the present case can be significantly larger than that in the corresponding Newtonian case; the former is more sensitive to the variation in the thickness of double layer than the latter, and the difference between the two increases with decreasing thickness of double layer. The shear-thinning effect is important under the following conditions: the double layer is thin, the boundary effect is important, and/or the aspect ratio is large. We show that increasing the aspect ratio can either raise or lessen its mobility, which is not found previously, and can play an important role in electrophoresis measurement.

Keywords Electrophoresis · Boundary effect · Rod in cylindrical microchannel · Carreau fluid

List of symbols

a	radius of rod, m
b	radius of microchannel, m
d	semi-length of rod, m
e	elementary charge, C
$\mathbf{e}_z$	unit vector in z-direction, dimensionless
E	strength of applied electric field, $m^2/V/s$
$\mathbf{E}$	applied electric field, V/m
F_D	hydrodynamic force acting on rod in z-direction, N
F_E	electric force acting on rod in z-direction, N
j	index of ionic species, dimensionless
k_B	Boltzmann constant, J/K
L_C	critical length of rod, m
L_T	critical length of microchannel, m
$\mathbf{n}$	unit normal vector on rod surface, dimensionless
n_j^0	bulk number concentration of ionic species j, $1/m^3$
N	power-law index of viscosity, dimensionless
p	hydrodynamic pressure, Pa
PD	percentage deviation of mobility, dimensionless
r	radial coordinate, m
S	rod surface, m^2
T	absolute temperature, K
$\mathbf{u}$	velocity of liquid phase, m/s
U	z-component of rod velocity, m/s
U_E	$=\varepsilon(k_BT/e)E/\eta$, m/s
z	axial coordinate, m
z_j	valence of ionic species j, dimensionless

Greek symbols

∇	gradient operator, 1/m
α	relaxation time constant for viscosity, s
ε	permittivity of liquid phase, $C^2/N/m^2$
ζ_p	surface potential of rod, V.
ζ_w	surface potential of microchannel, V
η	apparent viscosity, kg/m/s
η_0	zero-shear-rate viscosity, kg/m/s
$\dot{\boldsymbol{\gamma}}$	rate of strain tensor, 1/s
$\dot{\gamma}$	magnitude of rate of strain tensor, 1/s

L.-H. Yeh · J.-P. Hsu (✉)
Department of Chemical Engineering,
National Taiwan University, Taipei 10617, Taiwan
e-mail: jphsu@ntu.edu.tw

κ reciprocal Debye length, 1/m
λ $=a/b$, dimensionless
θ angular coordinate, dimensionless
μ^* scaled electrophoretic mobility, dimensionless
Ψ electrical potential, V
Ψ_1 electrical potential in the absence of applied electric field, V
Ψ_2 electrical potential outside rod arising from applied electric field, V

1 Introduction

Electrophoresis (Smoluchowski 1917) has been applied extensively in various fields of both fundamental and practical significance (Keh and Anderson 1985; Corradini 1997; Heller 2001; Ye et al. 2002; Liu et al. 2004; Davison and Sharp 2006; Hsu and Kuo 2006; Hsu and Yeh 2007a). On theoretical part, the available results in the literature are mainly based on Newtonian fluids; those based on non-Newtonian fluids are very limited due to the difficulty of solving the governing electrokinetic equations. Extending the analysis based on a Newtonian fluid to that on a non-Newtonian fluid, however, is highly desirable because many practical examples involve the latter case. The addition of polymer or surfactant to improve the stability of a colloidal dispersion (Hunter 1989a; Besra and Liu 2007), for example, can yield a shear-thinning fluid. These substances are also introduced as additives to the electrolyte solutions employed in protein or DNA capillary zone electrophoresis to minimize protein- or DNA-capillary wall interaction so that its performance can be are improved (Corradini 1997; Heller 2001). Note that if the concentration of dispersed particles is sufficiently high, the resulting dispersed system can be of non-Newtonian nature (Hunter 1989b). Several attempts have been made previously on the theoretical analysis of the electrophoresis in a shear-thinning Carreau fluid. Lee et al. (2003), for instance, made the first theoretical attempt on the analysis of the electrophoresis in a non-Newtonian fluid by considering a rigid sphere at the center of a spherical cavity filled with Carreau fluids under the conditions of low surface potential and weak applied electric field. Hsu et al. (2004a) and Hsu and Yeh (2007b) extended this analysis to the case where the sphere is at an arbitrary position in the cavity. The electrophoresis of a concentrated spherical dispersion in a Carreau fluid at low surface potentials was investigated by Hsu et al. (2004b), and that at arbitrary surface potentials studied by Lee et al. (2004). The electrophoresis of a rigid sphere normal to a planar surface was analyzed by Lee et al. (2005), that normal to a large disk by Hsu et al. (2007b), and that along the axis of a cylindrical pore by Hsu et al. (2006). A conclusion common to these studies is that the electrophoretic mobility of a particle in a shear-thinning fluid is larger than that in the corresponding Newtonian fluid.

In this work, previous study on the electrophoretic behavior of a spherical particle in non-Newtonian fluid is extended to the case of a cylindrical particle by considering the electrophoresis of a finite rod along the axis of a cylindrical microchannel. In practice, many inorganic and biological entities such as clay, protein, and DNA are better described by a rod-like particle. Typical application of the problem under consideration includes, for example, the separation of protein (Corradini 1997) and DNA (Heller 2001) through electrophoresis. The influences of the presence of the boundary, the aspect ratio of the particle, the thickness of double layer, and the nature of the dispersion medium on the electrophoretic behavior of the particle are investigated.

2 Theory

The problem under consideration is illustrated in Fig. 1, where a rigid, non-conducting rod of radius a and length $2d$ is driven by a uniform electric field $\mathbf{E}$ moving along the axis of a long, non-conducting, cylindrical microchannel of radius b. Let $\lambda = a/b$, which is a measure for the significance of the boundary effect. (r, θ, z) are the cylindrical coordinates with the origin at the center of the particle, and $\mathbf{E}$ is in the z-direction. The microchannel is filled with a shear-thinning Carreau fluid the viscosity of which, $\eta(\dot{\gamma})$, is described by (Yasuda et al. 1981; Bird et al. 1987)

$$\eta(\dot{\gamma}) = \eta_0[1 + (\alpha\dot{\gamma})^2]^{(N-1)/2} \tag{1}$$

where $\dot{\gamma}$ is the magnitude of the rate of strain tensor $\dot{\boldsymbol{\gamma}}$, $\eta_0 = \eta(\dot{\gamma} = 0)$, α is the relaxation time constant, and N is the power-law index. Carreau fluid has been proven to be a useful model to simulate non-Newtonian fluids for various polymeric systems, such as 1% methylcellulose Tylose in glycerol solution and 0.3% hydroxyethyl–cellulose Natrosol HHX in glycerol solution (Siska et al. 2005), and pure poly(ethylene oxide) (Hyun et al. 2001). In the separation of protein (Corradini 1997) and DNA (Heller 2001) through capillary electrophoresis, these polymers are utilized to improve selectivity and resolution.

If the applied electric field is relatively low to that established by the particle and/or the microchannel, the surface potential is low, the liquid is incompressible fluid, and the system is at a pseudo-steady state, then the electric field (Henry 1931) and the flow field (Bird et al. 1987) can be described by

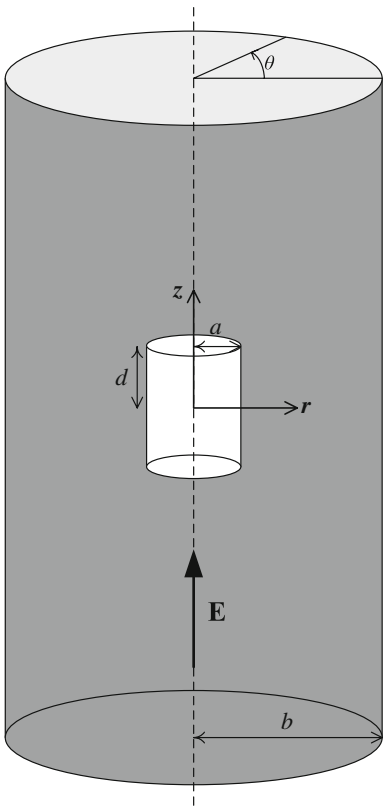

Fig. 1 The electrophoresis of a rigid, non-conducting rod of radius a and length $2d$ along the axis of a long, non-conducting cylindrical microchannel of radius b filled with a Carreau fluid. (r, θ, z) are the cylindrical coordinates with the origin at the center of the particle, **E** is a uniform applied electric field, which is in the z-direction

$$\nabla^2\Psi_1 = \kappa^2\Psi_1 \tag{2}$$

$$\nabla^2\Psi_2 = 0 \tag{3}$$

$$\nabla\cdot\mathbf{u} = 0 \tag{4}$$

$$\nabla\cdot[\eta(\dot{\gamma})\dot{\boldsymbol{\gamma}}] - \nabla p = \left\{\sum_j z_j e n_j^0 \exp[-z_j e\Psi/k_B T]\right\}\nabla\Psi_2 \tag{5}$$

In these expressions, ∇ and ∇^2 are the gradient operator and the Laplacian, respectively, and $\kappa = \left[\sum_j n_j^0 (ez_j)^2/\varepsilon k_B T\right]^{1/2}$ is the reciprocal Debye length. n_j^0, z_j, ε, e, k_B, and T are the bulk number concentration and the valence of ionic species j, the permittivity of the liquid phase, the elementary charge, the Boltzmann constant, and the absolute temperature, respectively. Ψ_1 denotes the electric potential in the absence of **E**, and Ψ_2 is the electric potential outside the particle arising from **E**; $\Psi = \Psi_1 + \Psi_2$, which is the electric potential of the system under consideration. **u** is the velocity of the liquid phase, and p is the pressure.

The following boundary conditions are assumed:

$$\Psi_1 = \zeta_p \text{ and } \mathbf{n}\cdot\nabla\Psi_2 = 0 \quad \text{on the particle surface} \tag{6}$$

$$\Psi_1 = \zeta_w \text{ and } \mathbf{n}\cdot\nabla\Psi_2 = 0 \quad \text{on the microchannel surface} \tag{7}$$

$$\Psi_1 = 0 \quad \text{and} \quad \nabla\Psi_2 = -\mathbf{E},\ |z|\to\infty,\ r<b \tag{8}$$

$$\mathbf{u} = U\mathbf{e}_z \quad \text{on the particle surface} \tag{9}$$

$$\mathbf{u} = 0 \quad \text{on the microchannel surface} \tag{10}$$

$$\mathbf{u} = 0,\ |z|\to\infty,\ r<b \tag{11}$$

In these expressions, ζ_p and ζ_w are the surface potential of the particle and that of the microchannel, respectively. **n** is the unit normal vector directed into the liquid phase, U the z-component of the particle velocity, and $\mathbf{e}_z$ the unit vector in the z-direction. Here, we assume that both the particle and the microchannel are non-conductive and impenetrable to ionic species, and their surfaces are no-slip. In practice, the linear size of a microchannel is on the order of 10–100 μm and that of a particle on the order of 1 μm. This implies that the continuum model represented in Eqs. (1)–(11) are realistic for problems of practical significance.

Under the conditions assumed, the forces acting on the particle include the electric force and the hydrodynamic force. To evaluate the velocity of the particle, only the z-components of these forces, F_E and F_D, need be evaluated. These forces can be obtained by integrating the Maxwell stress tensor (Hsu and Yeh 2006; Hsu et al. 2007a) and the hydrodynamic stress tensor (Backstrom 1999; Hsu et al. 2007a) over the particle surface. U is then determined from the relation $F_E + F_D = 0$ (Hsu and Kao 2002).

3 Results and discussion

Numerical simulation is conducted to examine the influences of the parameters key to the present problem, including the thickness of double layer, the aspect ratio of the rod, the relative size of the microchannel, the Carreau number ($\alpha U/a$), and the power-law index N, on the electrophoretic behavior of the particle. To this end, the governing equations and the associated boundary conditions are solved numerically by FlexPDE (version 2.22, PDE Solutions Inc., USA). This software was justified to be efficient and accurate for solving the problem of the present type (Hsu and Ku 2005; Hsu et al. 2006). We have shown previously that if the ratio (length of the computation domain in the axial direction/particle radius) exceeds ca. 10, the microchannel can be considered as sufficiently long, that is, its end effect is negligible (Hsu and Ku 2005). Grid independence is checked during numerical simulation

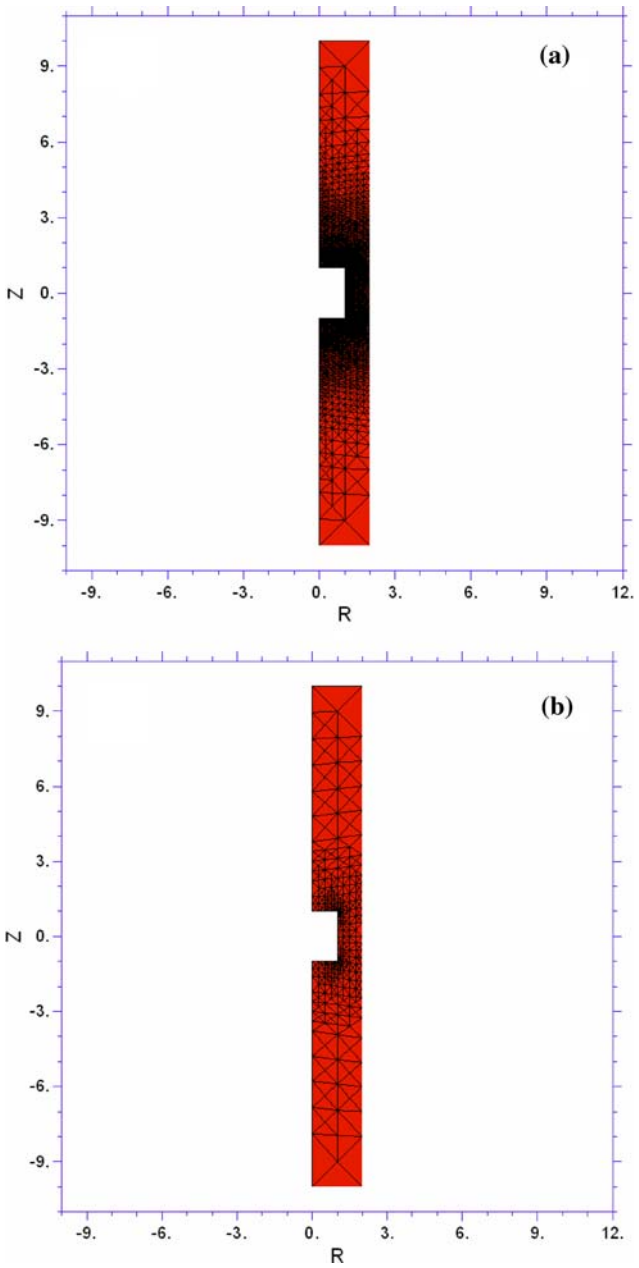

Fig. 2 Typical mesh used in the resolution of the electric field (**a**) and that of the flow field (**b**), the numbers of nodes are 21,235 and 1,476 in **a** and **b**, respectively

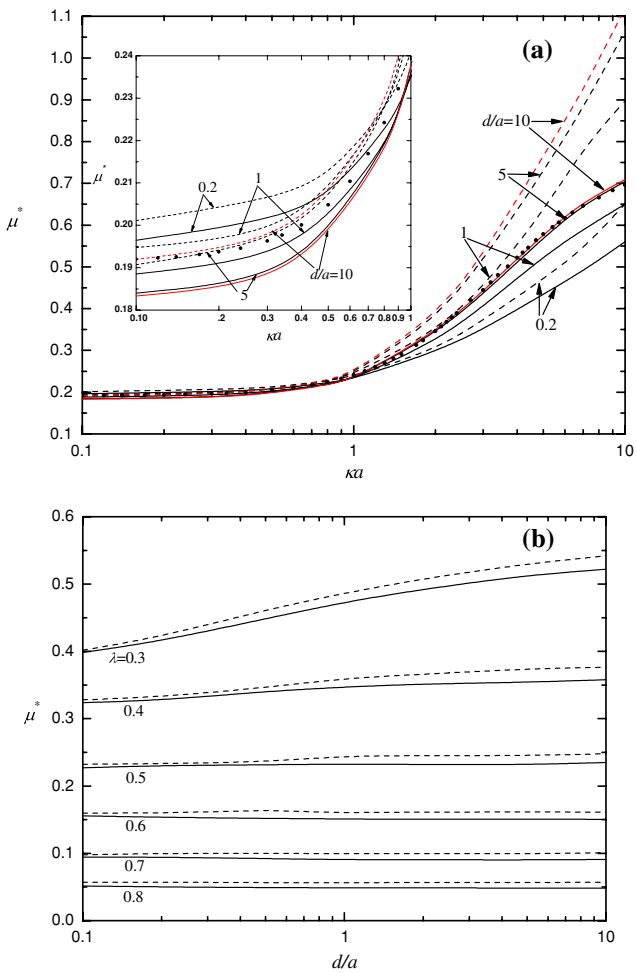

Fig. 3 Variation of the scaled electrophoretic mobility μ^* as a function of κa for various values of (d/a) (**a**), that as a function of (d/a) for various values of λ (**b**). $\lambda = 0.5$ in (**a**) and $\kappa a = 1$ in (**b**). *Solid curves* Newtonian fluid, *dashed curves* Carreau fluid with $N = 0.8$ and $\alpha U_E/a = 0.8$; discrete symbols, analytical results of Liu et al. (2004) for the case where $L_T/L_C = 100$

to ensure that the mesh used is appropriate. Figure 2 shows the typical mesh used where the numbers of nodes are 21,235 and 1,476 for the electric field and the flow field, respectively. For illustration, we assume that $\zeta_p = \kappa_B T/e$ is on the order of 25.4 mV and $\zeta_w = 0$. The former assumption assures that the linearized Poisson–Boltzmann equation, Eq. (2), is sufficiently accurate. An example where the latter assumption is realistic is a fused-silica pore with a hydrophobic coating like a cross-linked polyacrylamide or poly(vinyl alcohol) (Liu and Lee 2006). The assumption that $\zeta_w = 0$ implies that the effect of electroosmotic flow is negligible. In addition, the scaled mobility $\mu^* = U/U_E$ is used in subsequent discussion for a more concise representation where $U_E = \varepsilon(k_B T/e)E/\eta$ is a reference velocity. Note that a Newtonian fluid can be recovered as a special case of the present Carreau model by choosing $N = 1$ and/or $\alpha = 0$, and a power-law fluid can be obtained by choosing a sufficiently large α.

The influences of the thickness of double layer, measured by κa, the aspect ratio of the rod (d/a), and the relative size of the microchannel λ ($=a/b$) on the scaled electrophoretic mobility μ^* are illustrated in Fig. 3. For comparison, the results for the corresponding Newtonian fluid case and that of Liu et al. (2004), where the electrophoresis of a cylindrical particle in a Newtonian fluid in a long tube was analyzed, are also presented. Liu et al. (2004) considered the case where the end effect of the particle is negligible by assuming that it is sufficiently long

($a/L_C \ll 1$), and $L_T/L_C = 100$, L_C and L_T being the length of the particle and that of the tube, respectively. As seen in Fig. 3a, the result of Liu et al. (2004) is close to that of the present study at $d/a = 10$, implying that if (d/a) exceeds ca. 10, the particle can be considered as a one-dimensional rod. Note that, however, because the difference between the two is more significant at smaller κa (thicker double layer) that critical value is expected to be larger at smaller κa. As seen in Fig. 3, for both Newtonian and Carreau fluids, μ^* increases monotonically with increasing κa, and decreases monotonically with increasing λ. The former arises from the increase in the charge density on the particle surface, and the latter is due to the increase in the hydrodynamic drag arising from the presence of the microchannel (Hsu and Ku 2005; Hsu and Yeh 2007a, b). For Newtonian fluids, if κa is small (thick double layer) and/or λ is large (significant boundary effect), μ^* decreases with the increasing (d/a), but the opposite trend is observed if κa is large and/or λ is small. These behaviors arise from the competition between the hydrodynamic drag force and the electrical driving force acting on the particle as κa and/or λ vary (Hsu and Ku 2005). For the present case, the surface area of the particle increases with increasing (d/a), so are the amount of surface charge and the electrical driving force. However, the hydrodynamic drag force increases at the same time. If κa is small and/or λ is large, the rate of increase in the hydrodynamic drag force as (d/a) increases is faster than that in the electrical driving force, but the opposite occurs if κa is large and/or λ is small. Figure 3b shows that at large λ, μ^* is insensitive to the variation of (d/a), implying that if λ is large, although the hydrodynamic drag force dominates, it is offset considerably by the electrical driving force. It is interesting to note that the qualitative behaviors of μ^* as λ, κa, and (d/a) vary for the present Carreau fluid case are similar to those for the corresponding Newtonian fluid case only if (d/a) is sufficiently small (<5). Figure 3a reveals that for small κa if (d/a) is small, μ^* decreases with the increasing (d/a); but if (d/a) is sufficiently large, μ^* increases with increasing (d/a). This can be explained by that the larger the (d/a) the more significant the shear-thinning effect and at large (d/a) the qualitative behavior of μ^* is dominated by that effect, as will be justified later. The behavior of μ^* at different levels of (d/a) in the present Carreau fluid case is quite different from that in a Newtonian fluid (Sherwood 1982; Chen and Koch 1996; Hsu and Ku 2005), where μ^* decreases with increasing (d/a) (or κd) as $\kappa a \to 0$ (or $\kappa^{-1} \gg a$). Figure 3 also suggests that, for both Newtonian and Carreau fluids, the critical value of κa, κa_c, at which the qualitative trend of μ^* as (d/a) varies depends largely upon the levels of κa and λ. This is because that if the double layer is thicker than the width of the gap between the rod and the microchannel, $\kappa(b - a) < 1$ or $\kappa a < \lambda/(1 - \lambda)$, μ^* is insensitive to the variation in κa. That is, the double layer surrounding the rod is deformed by the microchannel wall, and the electrical driving force, which is much greater than the hydrodynamic drag force, depends weakly upon κa. As seen in Fig. 3a ($\lambda = 0.5$) $\kappa a_c \cong 1$ for a Newtonian fluid. Note that, if (d/a) is sufficiently small (≤ 5), due to the shear-thinning effect the κa_c of a Carreau fluid is smaller than that of the corresponding Newtonian fluid.

Let μ^*(Carreau) and μ^*(Newtonian) be the scaled mobility of a particle in the present Carreau fluid and that in the corresponding Newtonian fluid, respectively. The shear-thinning nature of the present Carreau fluid implies that μ^*(Carreau) $\geq$ μ^*(Newtonian). Define the percentage difference between the two, *PD*, as

$$\mathrm{PD} = \frac{|\mu^*(\mathrm{Carreau})| - |\mu^*(\mathrm{Newtonian})|}{|\mu^*(\mathrm{Newtonian})|} \times 100\% \qquad (12)$$

PD provides a measure for the significance of the shear-thinning effect of the present Carreau fluid. Figure 4 reveals that for the ranges of the parameters considered, PD

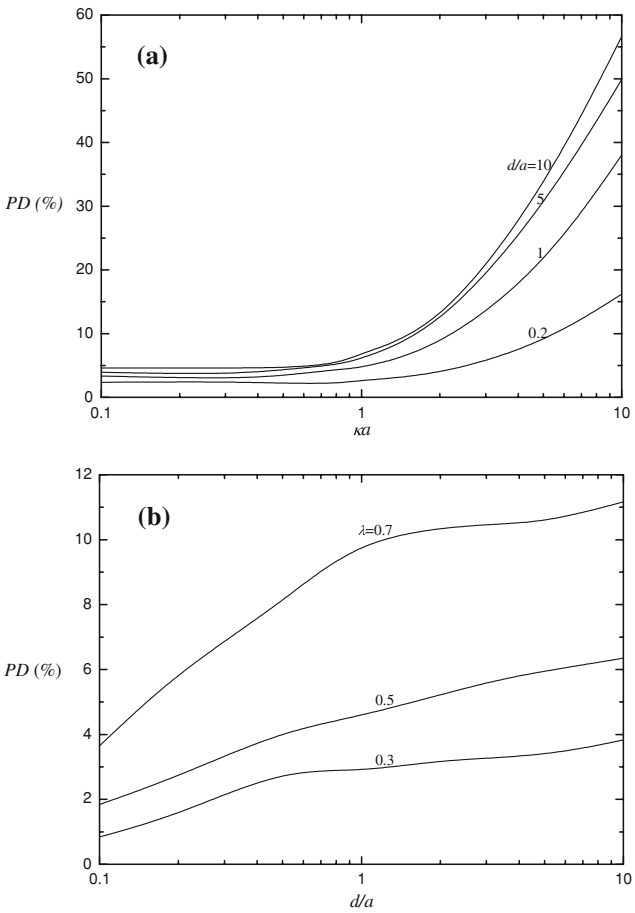

Fig. 4 Variation of percentage deviation in scaled electrophoretic mobility, PD = (|μ^*(Carreau)| − |μ^*(Newtonian)|)/|μ^*(Newtonian)| × 100%, for the cases of Fig. 3

can be on the order of 50%. In general, the shear-thinning effect is significant if κa is large (thin double layer), λ is large (boundary effect is important), and/or (d/a) is large (large aspect ratio); these can also be inferred from Fig. 3. Similar trends were also observed in other systems (Hsu et al. 2006; Hsu and Yeh 2007b). The dependence of the shear-thinning effect on κa is due to that μ^* increases with increasing κa, as pointed out in the discussion of Fig. 3, and can also be explained by the variation of the shear rate arising from the non-slip conditions assumed on the surfaces of the particle and the microchannel (Lee et al. 2003), as will be justified latter. The dependence of the shear-thinning effect on κa also explains the behavior of μ^* shown in Fig. 3a, where μ^*(Carreau) is seen to be more sensitive to the variation of κa than the corresponding μ^*(Newtonian) does and the difference between the two increases with increasing κa. The dependence of the shear-thinning effect on λ is due to that in the present case the flow field surrounding a particle is distorted by the microchannel, leading to a greater spatial variation in the shear rate than that for the case where the microchannel is absent. That on (d/a) and κa can be explained by the nature of the contours of $\eta^* = \eta/\eta_0$ illustrated in Fig. 5, where $\eta^* = 1$ corresponds to the case of a Newtonian fluid. This figure indicates that the spatial variation of η^* occurs mainly near the lateral surface of the particle, and the minimum of η^* occurs near its edge. This minimum increases with increasing κa and is insensitive to the

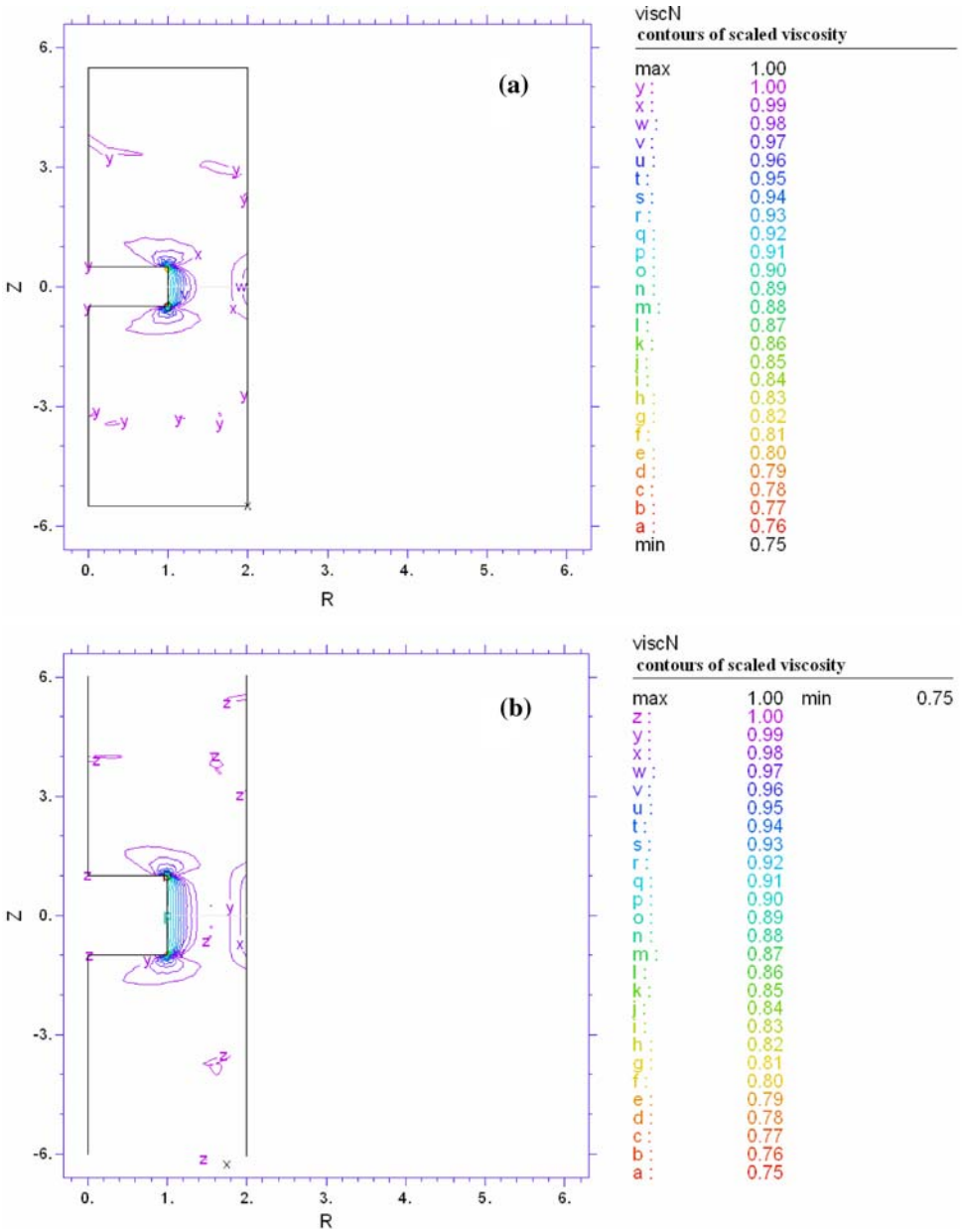

Fig. 5 Contours of the scaled viscosity η^*, viscN, for a Carreau fluid with $N = 0.8$ and $\alpha U_E/a = 0.8$ for the cases of Fig. 3 at $\lambda = 0.5$ where min, a, b, c…, max represent the levels of contours. **a** $d/a = 0.5$ and $\kappa a = 1$, **b** $d/a = 1$ and $\kappa a = 1$, **c** $d/a = 2$ and $\kappa a = 1$, **d** $d/a = 1$ and $\kappa a = 3$

Fig. 5 continued

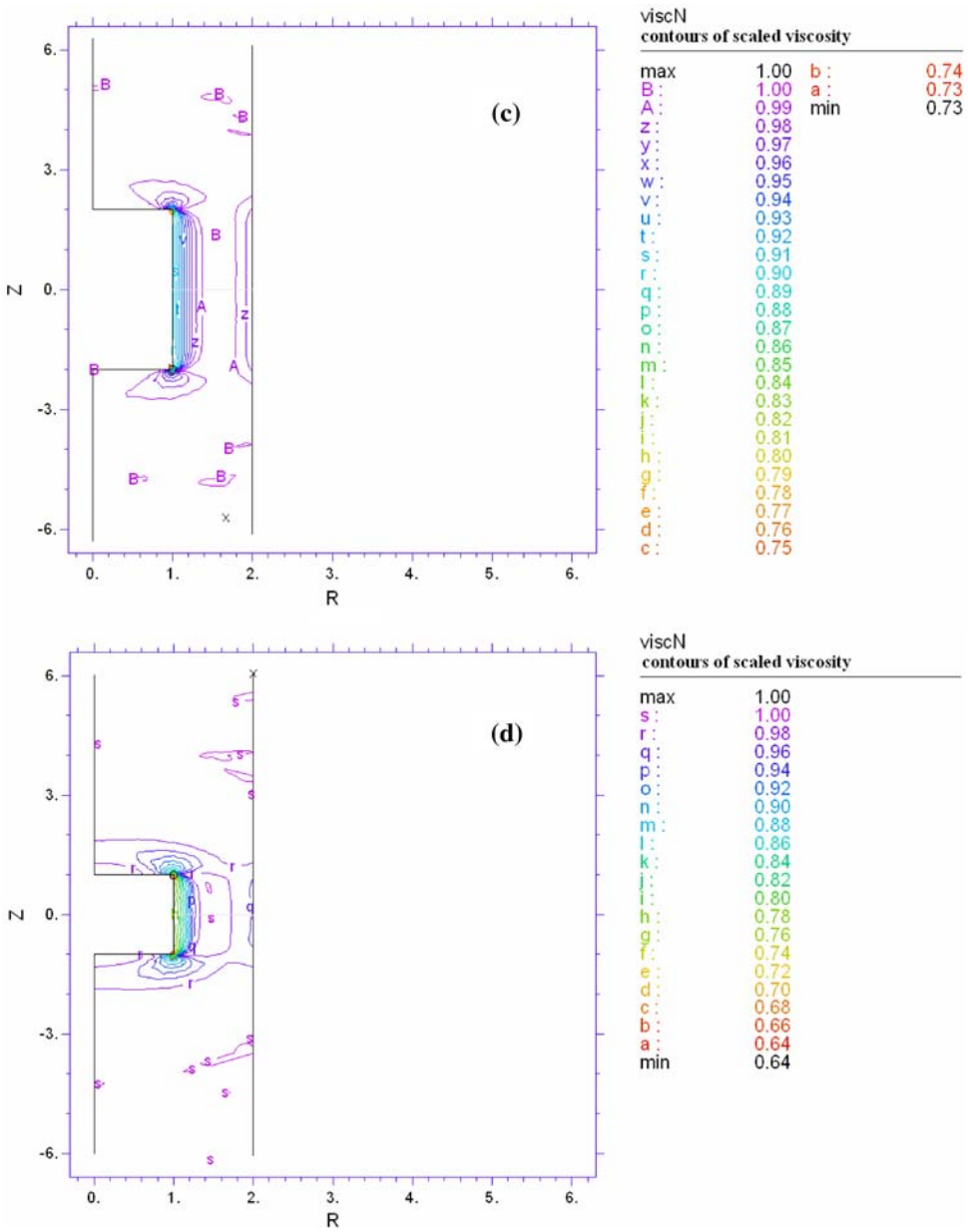

variation of (d/a). The latter implies that if κa is fixed, the shear-thinning effect is dominated by the magnitude of the lateral surface area of a particle. Because the larger the (d/a) the larger the lateral surface area, and, therefore, the more significant the shear-thinning effect, as observed in Fig. 4.

The influence of the nature of a Carreau fluid on the scaled mobility of a rod μ^* summarized in Figs. 6, 7, and 8 is consistent with the relevant theoretical results in the literature (Lee et al. 2003, 2004, 2005; Hsu et al. 2004a, b, 2006, 2007b; Hsu and Yeh 2007b), that is, the more significant the non-Newtonian nature of a fluid the larger the μ^*. In general, μ^* is more sensitive to the variation in ($\alpha U_E/a$) than to that in N, especially when κa is small. According to Figs. 6, 7, and 8, the following conditions lead to a larger μ^*: larger κa (thinner double layer), larger (d/a), and smaller λ (less significant the boundary effect). These are expected.

Figure 9 shows the variation of μ^* as a function of ($\alpha U_E/a$) for various values of (d/a) at two levels of κa. Here, the choice of the level of N is based on 1% methylcellulose Tylose in glycerol solution (N = 0.839, α = 0.296 s) (Siska et al. 2005) and pure poly(ethylene oxide) (N = 0.84, α = 4.37 s) (Hyun et al. 2001). As seen in Fig. 9a, if κa is sufficiently large (=1), μ^* increases monotonically with increasing (d/a) and/or ($\alpha U_E/a$). As illustrated in Fig. 9b, it is interesting to note that this is not the case when κa is small (=0.5). This figure reveals that, if ($\alpha U_E/a$) is sufficiently small, the variation of μ^* as (d/a) varies depends upon the level of (d/a). The insert of Fig. 9b indicates that

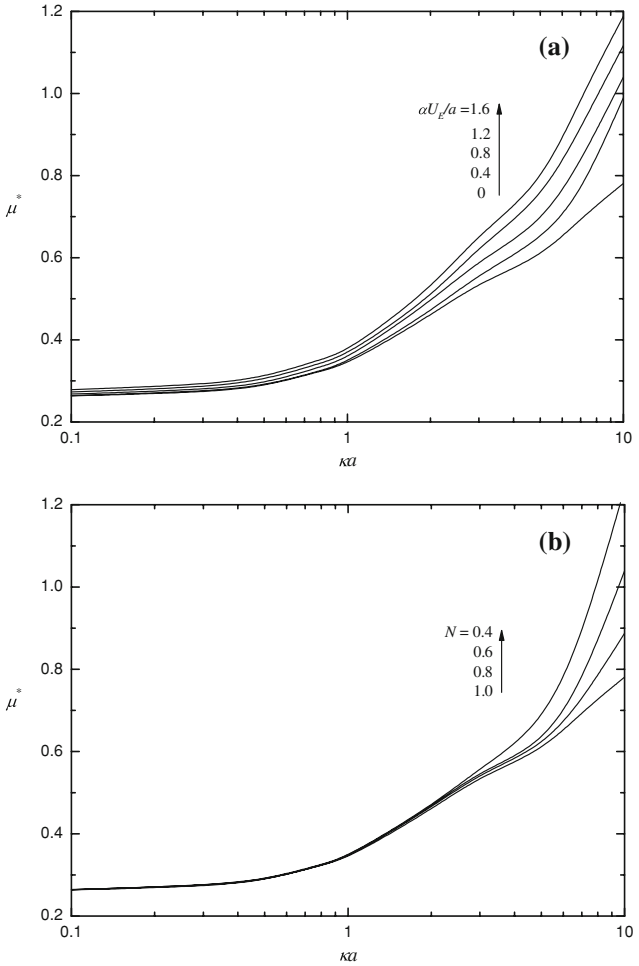

Fig. 6 Variation of the scaled electrophoretic mobility μ^* as a function of the κa for various values of ($\alpha U_E/a$) at $N = 0.8$ (**a**) and that at various values of N at $\alpha U/a = 0.2$ (**b**). Other parameters used are $\lambda = 0.4$, and $d/a = 1$

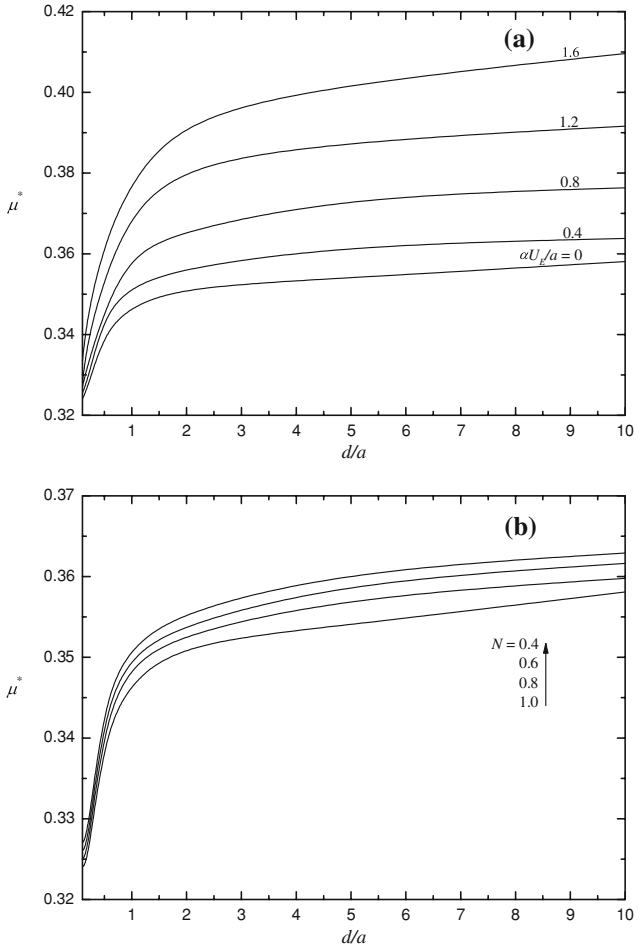

Fig. 7 Variation of the scaled electrophoretic mobility μ^* as a function of (d/a) for various values of ($\alpha U_E/a$) at $N = 0.8$ (**a**) and that at various values of N at $\alpha U/a = 0.2$ (**b**). Other parameters used are $\lambda = 0.4$ and $\kappa a = 1$

$\mu^*(d/a = 0.5) > \mu^*(d/a = 1) > \mu^*(d/a = 10) > \mu^*(d/a = 5)$, which is similar to the result shown in Fig. 3a. As seen in Fig. 9, if ($\alpha U_E/a$) is sufficiently large, μ^* increases monotonically with the increasing (d/a), as can be explained by that the larger the (d/a) the more significant the shear-thinning effect.

4 Conclusions

In summary, we studied the boundary effect on the electrophoretic behavior of a particle in a non-Newtonian fluid by considering the electrophoresis of a finite rod along the axis of a long cylindrical microchannel filled with a Carreau fluid. Under the conditions of weak applied electric field and low surface potential, the influences of the radius of the microchannel, the aspect ratio of the rod, the thickness of double layer, and the nature of the Carreau fluid on the mobility of the rod are investigated. The results of numerical simulation reveal that in general, due to the shear-thinning nature of the Carreau fluid, the mobility of the rod in the present case is larger than that in the corresponding Newtonian case. As in the Newtonian case, the mobility of the rod in the present case increases with decreasing double layer thickness, and decreases with increasing significance of boundary effect. The mobility in the present case is more sensitive to the variation of the thickness of double layer than that in the corresponding Newtonian case, and the difference between the two increases with decreasing thickness of double layer. For the ranges of the parameters considered, that difference can be on the order of 50%. The shear-thinning effect is important under the following conditions: the double layer is thin, the boundary effect is important, and/or the aspect ratio is large.

In the case of Newtonian fluids, the competition between the hydrodynamic drag and the electrical driving force acting on a rod leads to that if the double layer is

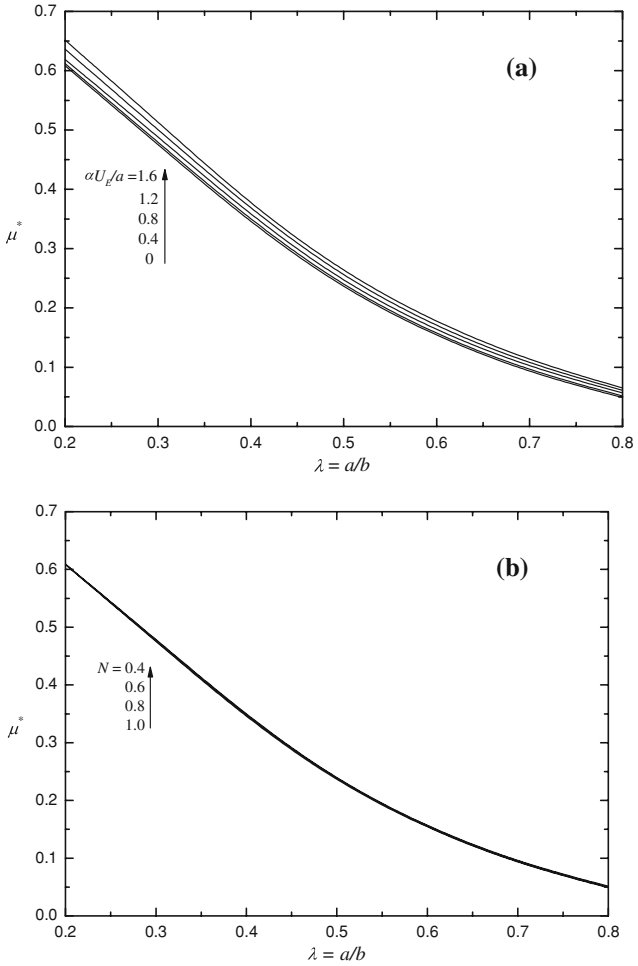

Fig. 8 Variation of the scaled electrophoretic mobility μ^* as a function of λ for various values of $(\alpha U_E/a)$ at $N = 0.8$ (**a**), and that at various values of N at $\alpha U/a = 0.2$ (**b**). Other parameters used are $d/a = 1$ and $\kappa a = 1$

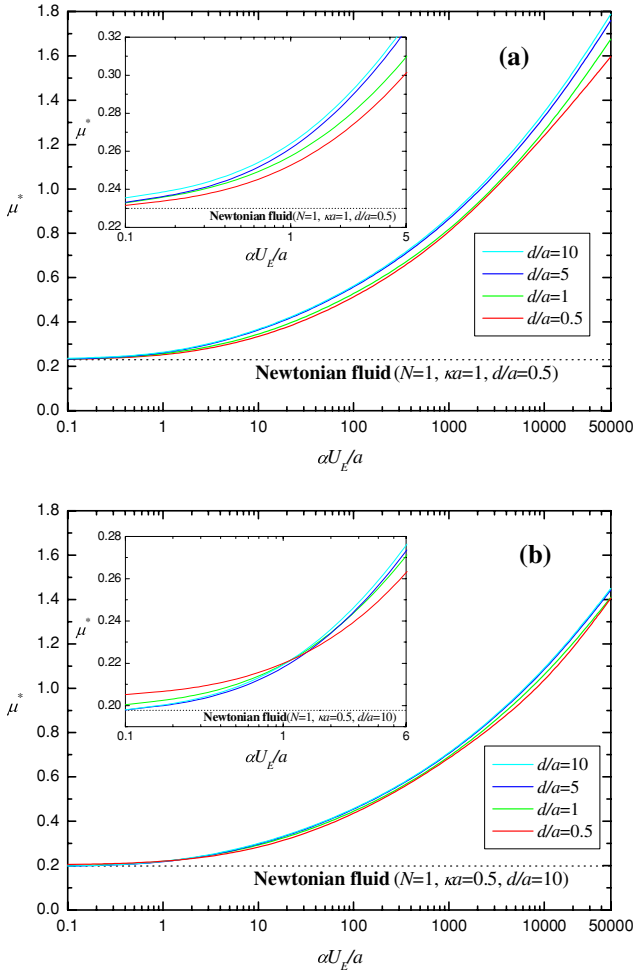

Fig. 9 Variation of the scaled electrophoretic mobility μ^* as a function of $(\alpha U_E/a)$ for various combinations of (d/a) and κa at $\lambda = 0.5$. **a** $\kappa a = 1$, **b** $\kappa a = 0.5$. *Solid curves* Carreau fluid with $N = 0.839$, *doted curves* Newtonian fluid for the case when $d/a = 0.5$ (**a**) and $d/a = 10$ (**b**)

thick and/or the boundary effect is significant, the mobility decreases with the increasing aspect ratio. The opposite trend is observed if the double layer is thin and/or the boundary effect is insignificant. However, this might not be the case if the microchannel filled with a Carreau fluid if the double layer is thick. If the nature of a Carreau fluid deviates only slightly from the corresponding Newtonian fluid, the mobility of a rod decreases with increasing aspect ratio, but the reverse trend is observed if the aspect ratio is sufficiently large. On other hand, if that deviation is significant, the mobility increases with increasing aspect ratio. These phenomena have not been reported in the literature.

The spatial variation of the fluid viscosity occurs mainly near the lateral surface of the rod, and the minimum of the viscosity occurs near its edge. This minimum increases with decreasing double layer thickness and is insensitive to the variation of the aspect ratio. The latter implies that if the thickness of double layer is fixed, the shear-thinning effect is dominated by the magnitude of the lateral surface area of the rod.

Acknowledgment This work is supported by the National Science Council of the Republic of China.

References

Backstrom G (1999) Fluid dynamics by finite element analysis. Studentlitteratur, Sweden

Besra L, Liu M (2007) A review on fundamentals and applications of electrophoretic deposition. Prog Mater Sci 52:1–61

Bird RB, Armstrong RC, Hassager O (1987) Dynamics of polymer liquids, vol I. Wiley, New York

Chen SB, Koch DL (1996) Electrophoresis and sedimentation of charged fibers. J Colloid Interface Sci 180:466–477

Corradini D (1997) Buffer additives other than the surfacant sodium dodecyl sulfate for protein separations by capillary electrophoresis. J Chromatogr B 699:221–256

Davison SM, Sharp KV (2006) Boundary effects on the electrophoretic motion of cylindrical particles: concentrically-positioned particles in a capillary. J Colloid Interface Sci 303:288–297

Heller C (2001) Principles of DNA separation with capillary electrophoresis. Electrophoresis 22:629–643

Henry DC (1931) The cataphoresis of suspended particles part I: the equation of cataphoresis. Proc R Soc London Ser A 133:106–129

Hsu JP, Kao CY (2002) Electrophoresis of a finite cylinder along a cylindrical pore. J Phys Chem B 106:10605–10609

Hsu JP, Ku MH (2005) Boundary effect on electrophoresis: finite cylinder in a cylindrical pore. J Colloid Interface Sci 283:592–600

Hsu JP, Kuo CC (2006) Electrophoresis of a finite cylinder positioned eccentrically along the axis of a cylindrical pore. J Phys Chem B 110:17607–17615

Hsu JP, Yeh LH (2006) Comparison of three methods for the evaluation of the electric force on a particle in electrophoresis. J Chin Inst Chem Eng 37:601–607

Hsu JP, Yeh LH (2007a) Electrophoresis of two identical rigid spheres in a charged cylindrical pore. J Phys Chem B 111:2579–2586

Hsu JP, Yeh LH (2007b) Electrophoresis of a charged boundary on electrophoresis in a Carreau fluid: a sphere at an arbitrary position in a spherical cavity. Langmuir 23:8637–8646

Hsu JP, Hung SH, Yu HY (2004a) Electrophoresis of a sphere at an arbitrary position in a spherical cavity filled with Carreau fluid. J Colloid Interface Sci 280:256–263

Hsu JP, Lee E, Huang YF (2004b) Electrophoresis of a concentrated dispersion of spherical particles in a non-Newtonian fluid. Langmuir 20:2149–2156

Hsu JP, Yeh LH, Ku MH (2006) Electrophoresis of a spherical particle along the axis of a cylindrical pore filled with a Carreau fluid. Colloid Polym Sci 284:886–892

Hsu JP, Yeh LH, Ku MH (2007a) Evaluation of the electric force in electrophoresis. J Colloid Interface Sci 305:324–329

Hsu JP, Yeh LH, Yeh SJ (2007b) Electrophoresis of a rigid sphere in a Carreau fluid normal to a large charged disk. J Phys Chem B 111:12351–12361

Hunter RJ (1989a) Foundations of colloid science, vol I. Oxford University Press, Oxford, pp 450–492

Hunter RJ (1989b) Foundations of Colloid Science, vol II. Oxford University Press, Oxford, pp 992–1050

Hyun YH, Lim ST, Choi HJ, Jhon MS (2001) Rheology of poly (ethyl oxide)/organoclay nanocomposites. Macromolecules 34:8084–8093

Keh HJ, Anderson JL (1985) Boundary effects on electrophoretic motion of colloidal spheres. J. Fluid Mech. 153:417–439

Lee E, Huang YF, Hsu JP (2003) Electrophoresis in a non-Newtonian fluid: sphere in a spherical cavity. J Colloid Interface Sci 258:283–288

Lee E, Tai CS, Hsu JP, Chen CJ (2004) Electrophoresis in a Carreau fluid at arbitrary zeta potentials. Langmuir 20:7952–7959

Lee E, Chen CT, Hsu JP (2005) Electrophoresis of a rigid sphere in a Carreau fluid normal to a planar surface. J Colloid Interface Sci 285:857–864

Liu JK, Lee ML (2006) Permanent surface modification of polymeric capillary electrophoresis microchips for protein and peptide analysis. Electrophoresis 27:3533–3546

Liu H, Bau H, Hu H (2004) Electrophoresis of concentrically and eccentrically positioned cylindrical particles in a long tube. Langmuir 20:2628–2639

Sherwood JD (1982) Electrophoresis of rods. J Chem Soc Faraday Trans 278:1091–1100

Siska B, Bendova H, Machac I (2005) Terminal velocity of non-spherical particles falling through a Carreau model fluid. Chem Eng Process 44:1312–1319

von Smoluchowski M (1917) Versuch einer mathematischen Theorie der Koagulationskinetik kolloider lösungen. Z Phys Chem 92:129–168

Yasuda K, Amstrong RC, Cohen RE (1981) Shear-flow properties of concentrated-solutions of linear and star branched polystyrenes. Rheol Acta 20:163–178

Ye C, Sinton D, Erickson D, Li D (2002) Electrophoretic motion of a circular cylindrical particle in a circular cylindrical microchannel. Langmuir 18:9095–9101